Diffusion-Assisted Aggregation and Synchronization in *Dictyostelium discoideum*

Seido Nagano

Fundamental Research Laboratories, NEC Corporation, 34 Miyukigaoka, Tsukuba, Ibaraki 305-8501, Japan

(Received 28 February 1997)

In biological pattern formation, chemotaxis and cell adhesion are essential. However, we lack quantitative data and a theory to understand their coordination. The cellular dynamics theory presented can clarify how *Dictyostelium discoideum* amoebae use diffusible cyclic adenosine 3′,5′-monophosphate, and coordinate chemotaxis and cell adhesion during aggregation. [S0031-9007(98)06173-0]

PACS numbers: 87.22.–q, 05.60.+w, 47.54.+r, 87.10.+e

Pattern formation is a fundamental phenomenon. *Dictyostelium discoideum* usefully models multicellular morphogenesis and pattern formation [1–3]. When bacterial food is available in the soil, unicellular amoebae grow and divide individually. When starved, they aggregate into a multicellular slug, and finally form a fruiting body, whose spores germinate into amoebae, completing the cycle. During aggregation, amoebae communicate by periodically producing and relaying cyclic adenosine 3′,5′-monophosphate (cAMP) signals. They also react chemotactically to cAMP and move towards the aggregation centers.

The cAMP oscillator in *Dictyostelium* includes the surface receptor (*R* or cARs), adenylate cyclase (AC), and cAMP phosphodiesterase (PDE). Binding of cAMP to the surface receptor activates AC, and cAMP is synthesized from intracellular adenosine triphosphate (ATP), then secreted by the cell. A few minutes later, the response ceases as the cells adapt to persistent stimulation. When the stimulus is removed, the cells resensitize, triggering the next cycle. The cAMP binding to cAR converts the *R* form of cAR to the modified *D* form [4].

Martiel and Goldbeter's (MG) [5] coupled kinetic rate law equations produced autonomous oscillation of cAMP within a cell. Later, Tyson *et al.* [6] introduced extracellular diffusion of cAMP for a homogeneous amoeba distribution. Levine *et al.* [7] and others [8–10], on the other hand, treated amoebae as having a continuous density, or as being based on the phenomenological-rule model [11]. Palsson and Cox [12] incorporated a PDE inhibitor by modifying the rate of cAMP decay. Oss *et al.* [13] and others [14–16] treated discrete amoebae by the nearest-neighbor or pointwise interaction. The effect of adaptation on cellular motion opposite to cAMP wave propagation was studied by Goldstein [17] and others [8–10]. Cell density models originally proposed by Keller and Segel [18] fail when the sharp boundary of a slug is formed because spatial derivatives of the cell density diverge at the boundary. Only a microscopic approach models both aggregation and slug formation.

Formation of an aggregate itself looks simple. However, there are still unanswered questions. First of all, how do individual amoebae judge where they should go when every amoeba is secreting cAMP at the same time to the extracellular medium as emergency calls? How do individual amoebae know the existence of others? It is known that the next stage of development is initiated when aggregation is complete. However, how do they know that there is already a sufficient number of amoebae within an aggregate? To answer these questions, we need a theory to study the intracellular biochemical reactions, cell-to-cell communication, and the cell movement in a consistent manner.

First, I generalize MG's equations as follows, so that I can accommodate the cell-to-cell communication.

$$\frac{d\gamma(\mathbf{x},t)}{dt} = \frac{k_t}{h}\,\beta(\mathbf{x},t) - k_e\gamma(\mathbf{x},t) + D\nabla^2\gamma(\mathbf{x},t), \quad (1)$$

$$\beta(\mathbf{x},t) = \sum_{j=1}^{N}\beta_j(t)\exp\Big[-\frac{4}{\sigma_0^2}(\mathbf{x}-\mathbf{x}_j)^2\Big], \quad (2)$$

$$\frac{d\beta_j}{dt} = \phi(\rho_j,\gamma_j) - (k_i + k_t)\beta_j, \quad (3)$$

$$\frac{d\rho_j}{dt} = f_2(\gamma_j)(1-\rho_j) - f_1(\gamma_j)\rho_j, \quad (4)$$

$$f_1(\gamma_j) = \frac{k_1 + k_2\gamma_j}{1+\gamma_j}, \qquad f_2(\gamma_j) = \frac{k_{-1} + 10k_{-2}\gamma_j}{1+10\gamma_j}, \quad (5)$$

$$\phi(\rho_j,\gamma_j) = 1800\,\frac{0.0001 + Y_j^2}{0.2575 + Y_j^2}, \qquad Y_J = \frac{\rho_j\gamma_j}{1+\gamma_j}. \quad (6)$$

The cAMP signal sources (β_j) of the MG type, described by Eqs. (3)–(6), are spatially distributed, and interact only through extracellular cAMP (γ) diffusion. The two-dimensional delta function can be expressed as $\delta(\mathbf{x}) = \lim_{\sigma_0\to 0} 4/\pi\sigma_0^2 \exp(-4\mathbf{x}^2/\sigma_0^2)$. Here, to derive Eqs. (1) and (2), I keep the diameter of an amoeba σ_0 finite instead of taking a limit and rewrite $4/\pi\sigma_0^2 h$ as $1/h$ since h is a free parameter. Adoption of a Gaussian function to describe a discrete amoeba has a clear advantage numerically since it does not have any singularity in it. Besides, intracellular biochemical reactions can be confined

 0031-9007/98/80(21)/4826(4)$15.00

within the localized cell body. In the above equations, γ and β_j, respectively, are the extracellular and intracellular concentrations of cAMP, and both are normalized by the cAMP dissociation constant $K_R = 10^{-7}M$; $\gamma_j = \gamma(\mathbf{x}_j, t)$; ρ_j is the fraction of the receptor in the active states of the jth amoeba; $\sigma_0 = 10$ μm is the diameter of an amoeba; $\mathbf{x}_j$ are two-dimensional amoeba position vectors; N is the total number of amoebae; $k_e = 5.4\ \text{min}^{-1}$, $k_i = 1.7\ \text{min}^{-1}$, and $k_t = 0.9\ \text{min}^{-1}$, respectively, are rate constants for the extracellular PDE, intracellular PDE, and cAMP transport into the extracellular medium; and $k_1 = 0.036\ \text{min}^{-1}$, $k_{-1} = 0.36\ \text{min}^{-1}$, $k_2 = 0.666\ \text{min}^{-1}$, and $k_{-2} = 0.003\,33\ \text{min}^{-1}$ are rate constants for the modification of the receptors. The parameter values are the same as those used by MG except that $h = 0.104$ and the diffusion constant of cAMP $D = 4.0 \times 10^{-4}\ \text{cm}^2/\text{s}$ [19], where the parameter h was originally introduced as the ratio of extracellular to intracellular volume by MG. With these parameters, we can reproduce the MG oscillator modes within a cell.

To simulate aggregation, however, I need information not only about the cell-to-cell communication, but also about the cell adhesion force and the chemotaxis. Amoebae rapidly synthesize adhesive glycoproteins in their cell membranes after starvation [20], and become increasingly adhesive. Cell interaction potential,

$$v_{m-n}(r) = \epsilon_0 \frac{mn}{m-n}\left[\frac{1}{m}\left(\frac{\sigma_0}{r}\right)^m - \frac{1}{n}\left(\frac{\sigma_0}{r}\right)^n\right], \quad (7)$$

may describe this short-range cell adhesion force. It has a minimum value $-\epsilon_0$ at $r = \sigma_0$ for any m, n integer pairs. The short-range force operates only when amoebae come very close to each other. A stable structure is formed when they touch. Numerical values for ϵ_0, m, and n must be determined experimentally. Since we do not know the quantitative relationship between the cAMP concentration and chemotactic response [21], I assume that the long-range chemotactic force is proportional to the gradient of the extracellular cAMP (γ), which enables me to handle the fast diffusible cAMP field and the slow movement of the amoebae consistently. Then, the equations of motion for amoebae become

$$m_a \frac{d^2\mathbf{x}_i}{dt^2} = \epsilon_1 \nabla_i \gamma(\mathbf{x}_i, t) - \sum_{j(\neq i)}^{N} \nabla_i v_{m-n}(|\mathbf{x}_i - \mathbf{x}_j|) - \eta \frac{d\mathbf{x}_i}{dt}, \quad (8)$$

where the last term on the right-hand side of the equation describes the frictional force due to the substrate, and $m_a = 10^{-9}$ g is the mass of an amoeba. Friction dissipates the kinetic energy of amoebae to form a final stable aggregate. The coupled equations (1)–(8) can handle chemotaxis, cell adhesion, and cell-to-cell communication consistently. The time evolution of aggregation shown in Fig. 1 clarifies the physics of the theory,

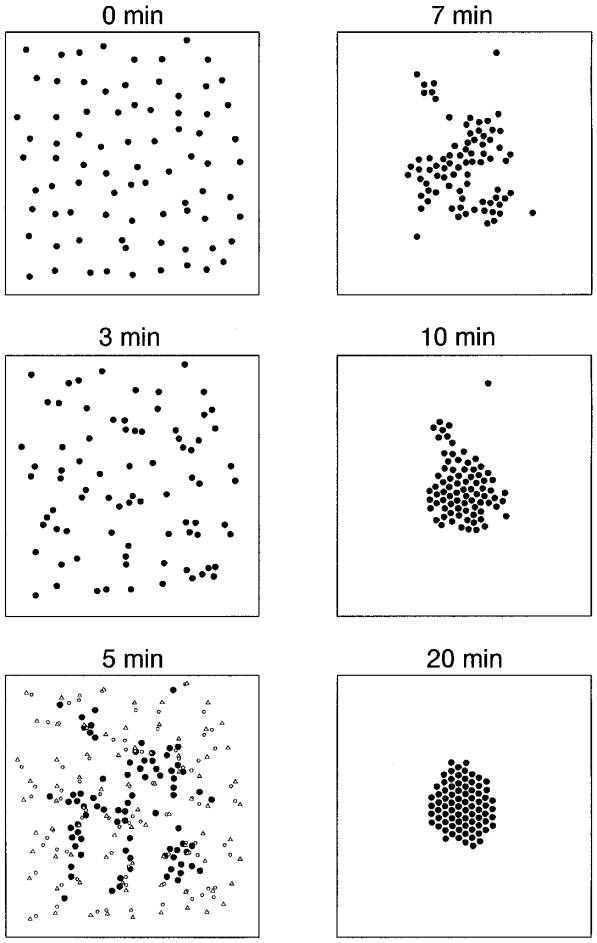

FIG. 1. Time development of 80 amoebae in a $30\sigma_0 \times 30\sigma_0$ area, where σ_0 is the diameter of an amoeba. At $t = 5$ min, the amoeba distributions at $t = 0$ min (Δ) and at $t = 3$ min ($\bigcirc$) are superimposed to clarify the spiral and stream pattern formations.

where $\epsilon_0 = 10^{-13}\ \text{g nm}^2/\text{min}^2$, $m = 9$, $n = 3$, $\epsilon_1 = (10^{-17}\ \text{g mm/min})K_R\sigma_0^3$, $\eta = 0.5$ g mm/min, and $N = 80$ in an area $30\sigma_0 \times 30\sigma_0$, with a time step of 0.005 min and a space unit of $\sigma_0/3 \simeq 0.0033$ mm to obtain convergence. Different combinations of m, n pairs did not produce qualitative changes in aggregation. Here, I have used the Fourier expansion method [22] using 8281 plane waves to solve Eq. (1). The initial random distribution was prepared according to a molecular dynamics method using Eq. (7) as an interaction potential to avoid overlapping amoeba. We recognize an aggregate formation after the spiral and stream patterns have formed.

To distinguish clearly the roles of the chemotaxis and adaptation during this aggregation, I conducted the following simulations, too. In the first case, I used only Eqs. (7) and (8) by setting $\epsilon_1 = 0$. This corresponds to the case without chemotaxis. In the second case, I used Eqs. (1)–(8), but by setting the right-hand sides of Eqs. (3) and (4) to zeros. This corresponds to the case without adaptation but with chemotaxis. Namely, intracellular oscillatory cycles

are killed. Without chemotaxis and adaptation amoebae have a tendency to form many small clusters before the completion of aggregation. A similar tendency of clustering without streams can be found by expanding the simulation area using the same number of amoebae.

To further clarify the physics underlying the present theory, I rewrite Eq. (8) as follows:

$$m_a \frac{d^2\mathbf{x}_i}{dt^2} = -\nabla_i U(\mathbf{x}_i, t) - \eta \frac{d\mathbf{x}_i}{dt}, \tag{9}$$

where

$$U(\mathbf{x}_i, t) = -\epsilon_1 \gamma(\mathbf{x}_i, t) + \frac{1}{2} \sum_{i \neq j}^{N} \upsilon_{m-n}(|\mathbf{x}_i - \mathbf{x}_j|). \tag{10}$$

That is, fast-moving extracellular cAMP and cell adhesion interactions form the time-dependent potential field for amoebae given by Eq. (10). Losing kinetic energy to friction until they reach a stable structure in the potential, amoebae fall into that potential. The ratio of ϵ_1 and ϵ_0 controls the balance of the two forces in the potential. For a given ϵ_1 and ϵ_0, the first term in $U(\mathbf{x}_i, t)$ becomes larger as the extracellular cAMP concentration increases, and the cAMP flow controls the amoeboid movement, and, as a consequence, streams are formed. For low extracellular cAMP concentrations, on the other hand, the second term dominates, and relative amoeba movement is enhanced, destroying the streams.

To investigate the cell-to-cell communication in more detail, I conducted several other kinds of numerical experiments. In Fig. 2, three amoebae are equally spaced σ_0 apart, and the signal initiation is at times $t = 0$, $t = 5$, and $t = 20$ min for amoebae A, B, and C, respectively. We can see that the synchronization of the cAMP pulses is achieved before the completion of the next cycle of cAMP pulses. The coupling of the extracellular cAMP leads to the amplitude and frequency modulations in the intracellular cAMP and in the fraction of the receptor in the active state. When many amoebae come closer together, a qualitative change in the frequency modulation is achieved. That is, the intracellular cAMP level no longer reaches zero, and it approaches the quasisteady level. This is consistent with the experimental results [2].

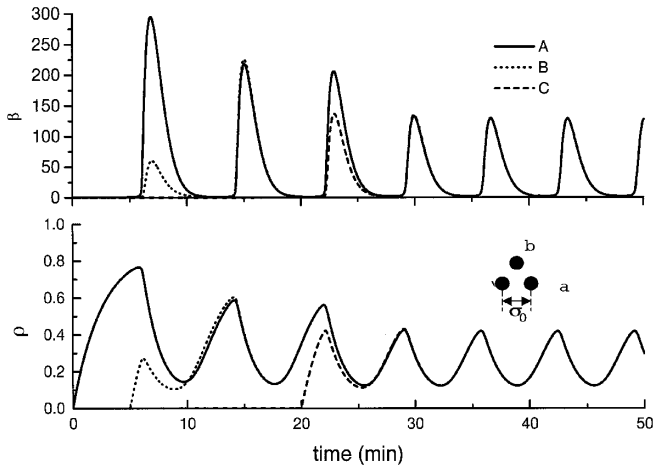

FIG. 2. Intracellular cAMP (β) and active-state fraction of the receptor (ρ), where amoebae A, B, and C initiated signal oscillations at $t = 0$, 5, and 20 min, respectively.

When many amoebae come close together, their internal cAMP production is reduced; however, when some amoebae are removed from the group, the internal cAMP production of the remaining amoebae increases so that the extracellular cAMP density remains the same. This clearly demonstrates that the synchronization of the cAMP oscillators is essential for adaptation and robustness in *Dictyostelium*. This is also consistent with the experimental observations of the *gbf* null cells [23,24]. In *Dictyostelium*, external information is being translated into internal information in this way through the synchronization procedure.

For simplicity, I choose η so that an aggregate has no kinetic energy left after its formation. A smaller η reproduces observed cellular motion within a slug although more detailed investigation is definitely needed. Dissipative aggregation resembles two-dimensional crystal growth [25]. Changes in cAMP secretion in response to the density changes and secretion providing chemotaxis resembles annealing.

The strategy adopted by *Dictyostelium* for pattern formation may be briefly summarized as follows. (i) *Dictyostelium* synchronize oscillatory cAMP signaling through the combination of extracellular cAMP diffusion and intracellular nonlinear cAMP production cycles. Coherent production efficiently relays the signal over a large area. (ii) Temporary aggregation centers formed by extracellular cAMP diffusion guide amoeboid movement. The slow movement of amoebae and the fast diffusion of extracellular cAMP continue to prevent metastable configurations. (iii) Changes in the intracellular cAMP productions brought about by the coupled nonlinear cAMP oscillators determine when amoebae initiate the next stage of development.

Historically, Turing [26] discovered that a spatial pattern can be formed if two substances with different diffusion rates react with each other, which is well known as the reaction-diffusion theory. This concept has been further developed as the activator-inhibitor theory and has been applied to many biological systems [27]. However, these theories treat two substances as continuous variables since they are based on the diffusion equations. Equations (1)–(8) reproduce experimentally observed pattern formation using discrete simplified amoebae without three-dimensional changes in cell shape [28]. Amoeboid movement and internal biochemical reactions are considered consistently with a reaction-diffusion equation for the diffusible molecules.

The study of the synchronization of coupled and spatially distributed oscillators has a long history dating back

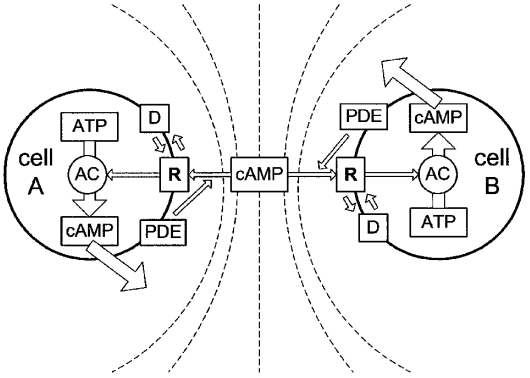

FIG. 3. Schematic view of the diffusion-assisted synchronization procedure; *R*: surface receptor, AC: adenylate cyclase, PDE: cAMP phosphodiesterase.

to the era of Huygens who recognized the synchronization of two clocks on the wall in the 17th century [29]. Similar phenomena have been found in many biological systems such as the flashing of fireflies [30]. Many former theoretical approaches to the synchronization of coupled oscillators may be roughly divided into two categories: one is phase-coupled model based [31] and the other is reaction-diffusion equation based. The phase-coupled model is a weak coupling approximation. The latter case can be further subdivided into local coupling approximation [32] and global coupling approximation [33,34] (where each oscillator is coupled with others of equal strength).

Equation (1) is a reaction-diffusion equation. However, the above limiting approximate approaches cannot be adopted here because for a given diffusion coefficient of cAMP amoebae must move from the weak coupling domain to the strong coupling domain continuously during aggregation. Furthermore, as can be seen from Fig. 2, both the frequency and amplitude of synchronized cAMP oscillators are significantly different from those of the original oscillators. This means that the basic assumptions of the phase-coupled model is not satisfied here, either. In this Letter, I have clarified how extracellular cAMP diffusion is used to synchronize signal oscillations between amoebae without the above limiting approximations (Fig. 3).

I thank Professor Urushihara and Professor Tanaka of the University of Tsukuba, Professor Loomis of UCSD, and Dr. Miwa, Dr. Nishiwaki, and Dr. Tabuse of NEC for their helpful discussions. Special thanks are also due to Dr. Ohta and Dr. Igarashi of NEC for their patient support.

Note added.—After submitting this manuscript, a paper by Wang and Kuspa [35] appeared. They observed both aggregation and mound formation in the absence of cAMP. Common qualitative similarities such as longer aggregation time and a critical cell density for aggregation exist in both cases. I plan to conduct a more detailed investigation in the near future.

[1] W. F. Loomis, *Dictyostelium Discoideum* (Academic Press, New York, 1975).
[2] R. A. Firtel, Genes Dev. **9**, 1427 (1995); Curr. Opin. Genet. Dev. **6**, 545 (1996).
[3] K. J. Lee, E. C. Cox, and R. E. Goldstein, Phys. Rev. Lett. **76**, 1174 (1996).
[4] P. N. Devreotes and J. A. Sherring, J. Biol. Chem. **260**, 6378 (1985).
[5] J. Martiel and A. Goldbeter, Biophys. J. **52**, 807 (1987).
[6] J. J. Tyson, K. A. Alexander, V. S. Manoranjan, and J. D. Murray, Physica (Amsterdam) **34D**, 193 (1989).
[7] H. Levine and W. Reynolds, Phys. Rev. Lett. **66**, 2400 (1991).
[8] B. N. Vasiev, P. Hogeweg, and A. V. Panfilov, Phys. Rev. Lett. **73**, 3173 (1994).
[9] T. Höfer, J. A. Sherratt, and P. M. Maini, Physica (Amsterdam) **85D**, 425 (1995).
[10] Y. Tang and H. B. Othmer, Math. Biosci. **120**, 25 (1994).
[11] D. Kessler and H. Levine, Phys. Rev. E **48**, 4801 (1993).
[12] E. Palsson and E. C. Cox, Proc. Natl. Acad. Sci. U.S.A. **93**, 1151 (1996).
[13] C. V. Oss, A. V. Panfilov, P. Hogeweg, F. Siegert, and C. J. Weijer, J. Theor. Biol. **181**, 203 (1996).
[14] H. Parnas and L. A. Segel, J. Cell Sci. **25**, 191 (1977).
[15] S. A. Mackay, J. Cell Sci. **33**, 1 (1978).
[16] O. O. Vasieva, B. N. Vasiev, V. A. Karpov, and A. N. Zaikin, J. Theor. Biol. **171**, 361 (1994).
[17] R. E. Goldstein, Phys. Rev. Lett. **77**, 775 (1996).
[18] E. F. Keller and L. A. Segel, J. Theor. Biol. **26**, 399 (1970).
[19] M. Dworkin and K. H. Keller, J. Biol. Chem. **252**, 864 (1977).
[20] W. Loomis, Microbiol. Rev. **60**, 135 (1996).
[21] F. Alcantara and M. Monk, J. Gen. Microbiol. **85**, 321 (1974).
[22] S. Nagano, Phys. Lett. A **156**, 493 (1991).
[23] S. K. Mann and R. A. Firtel, Proc. Natl. Acad. Sci. U.S.A. **86**, 1924 (1989).
[24] G. R. Schnitzler, C. Briscoe, J. M. Brown, and R. A. Firtel, Cell **81**, 737 (1995).
[25] B. J. Alder and T. E. Wainwright, Phys. Rev. **127**, 352 (1962).
[26] A. Turing, Philos. Trans. R. Soc. London B **237**, 37 (1952).
[27] A. J. Koch and H. Meinhardt, Rev. Mod. Phys. **66**, 1481 (1994).
[28] D. Wessels, H. Vawterhugart, J. Murray, and D. R. Soll, Cell Motil. Cytoskeleton **27**, 1 (1994).
[29] C. Huygens, *Hologium Oscillatorium* (F. Muguet, Paris, 1673), p. 117.
[30] J. Buck and E. Buck, Nature (London) **211**, 562 (1966).
[31] Y. Kuramoto, *Chemical Oscillations, Waves, and Turbulence* (Springer, Berlin, 1984).
[32] M. C. Cross and P. C. Hohenberg, Rev. Mod. Phys. **65**, 851 (1993).
[33] V. Hakim and W. J. Rappel, Phys. Rev. A **46**, R7347 (1992).
[34] N. Nakagawa and K. Kuramoto, Prog. Theor. Phys. **89**, 313 (1993); Physica (Amsterdam) **80D**, 307 (1995).
[35] B. Wang and A. Kuspa, Science **277**, 251 (1997).